



Mixers in Microwave Systems (Part 1)

Mixers continue to play a critical role in RF and microwave systems that employ frequency conversion. Although much has been written concerning the theory and operation of mixers, the purpose of this article is to present some highlights of these details as they relate to passive mixer design, theory, realization, and usage.

MIXER THEORY

To achieve frequency conversion, a periodic signal having frequency, f_R , is modulated by a periodic conductance (or resistance) waveform having frequency, f_L . The current resulting from the RF voltage being modulated by the fundamental component of the conductance waveform contains the sum and difference IF products: $f_R + f_L$ and $f_R - f_L$ or $f_L - f_R$. The other undesired currents generated are intermodulation products having frequencies of $n f_L \pm f_R$, where n is an integer. Inter-modulation products have also been referred to as idlers. In the case of an active mixer, one having conversion gain, the conductance waveform is that of one or more transistors. In the case of a passive mixer, which has conversion loss, the conductance waveform is generally that of one or more Schottky-barrier diodes. Increasingly, however, MESFET devices have been used instead of diodes to achieve wider dynamic range in passive mixers.

Analysis of the frequency conversion properties of mixers is non-trivial. The simplest model, which perhaps gives the best intuitive understanding of the mixing process is the linear phase-reversal mixer [1].

This model assumes the diode is nonreactive and acts as a linear rectifier, having a square-wave resistance waveform with zero forward and infinite backward resistances. The mixer is considered linear because the values of the circuit elements, including diode conductance, are independent of RF and LO levels. It has been shown that this model approxi-

mates the Schottky diode mixer closely enough to formulate theoretical limits for conversion-loss and intermodulation suppression [2, 3]. Figure 1 shows a conventional double-balanced diode mixer. During positive LO cycles, diodes D1 and D2 are turned on while D3 and D4 are off. The opposite is the case during negative LO cycles. This causes the RF (signal) voltage as seen by the IF port to change phase by 180 degrees every time the LO signal changes polarity. This can be represented mathematically by multiplying the sinusoidal signal voltage with the Fourier series for the square-wave switching function:

$$V_{out} = V_{RF} \sin(\omega_R t) \left[\frac{4}{\pi} \sum_{n=1,3,5,\dots} \frac{1}{n} \sin(n\omega_L t) \right] \tag{1a}$$

$$= V_{RF} \frac{4}{\pi} \left\{ \frac{1}{2} [\sin(\omega_L - \omega_R)t - \sin(\omega_R + \omega_L)t] + \frac{1}{6} [\sin(3\omega_L - \omega_R)t - \sin(3\omega_L + \omega_R)t] + \dots \right\} \tag{1b}$$

Conversion loss is equal to the reciprocal of conversion gain, and is defined as:

$$L = \frac{\text{Available RF Input Power}}{\text{Available IF Output Power}} \tag{2}$$

and RF-to-IF conversion loss is given by:

$$L = 20 \log \frac{V_{RF}}{V_{IF}} \tag{3} \\ = -20 \log \frac{2}{\pi} = 3.92 \text{ dB}$$

The $2/\pi$ term is the ratio of the signal voltage

to IF voltage. Equations 1 through 3 assume that the RF and IF ports are conjugately matched, all intermodulation (IM) products are resistively terminated, and no parasitic resistive or reactive losses exist. The above analysis has been generalized to show that when matched loads are presented to each IM product, and the RF, IF, and image signals are conjugately matched, the theoretical minimum conversion loss is 3.92 dB. Also, when all IM products and the sum ($f_L + f_R$) product are reactively terminated, the IF is conjugately

matched, and the RF and image signals are identically terminated, then the theoretical minimum conversion loss is 3 dB, with the lost energy equally divided between conversion to the image, and reflection-loss at the signal frequency [3]. The image, in this context, is a mixer-generated product having a frequency of $2f_L - f_R$. As discussed later in this paper, in the context of image-rejection, the image refers to noise or signal power having frequency, $2f_L - f_R$, that enters the mixer along with the RF signal. Idlers are intermodulation products that are associated with each mixer-generated LO harmonic. Idlers of order n comprise the two sidebands that are adjacent to each LO harmonic, and have frequencies of $f_n = n f_L \pm f_{IF}$, where n are integers greater than one. Figure 2 shows that the spectrum of signals present in a mixer includes the LO, IF, image, LO harmonics, and idlers [4].

SUMMARY OF MIXER ANALYSIS METHODS

The classical analysis of frequency conversion is given by Torrey and Whitmer [5] for a single exponential diode with small-signal RF and large signal LO voltages applied. The analysis considers the RF, IF, and image signals to be at low levels compared with the LO. This allows these three signals to be considered as variations of the LO voltage and current harmonics. The result is that their voltage and current waveforms are linearly

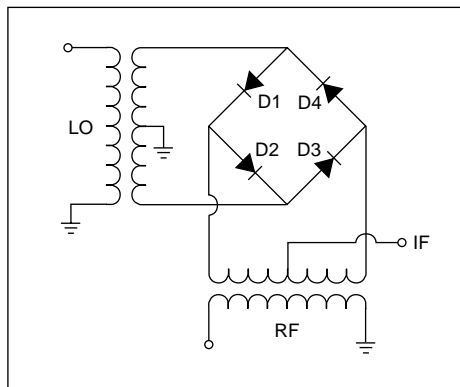


Figure 1. Schematic diagram of a double-balanced diode mixer.



related through an admittance matrix representing the mixer, with conversion loss being given as a function of diode conductance. The mixer can thus be regarded as a linear network with separate terminals at the RF, image, and IF frequencies. Theoretical minimum conversion loss is shown to be about 3.9 dB for the case where signal and image frequencies are terminated in the same resistance, and about 2.5 dB for the case where the image is short or open circuited. These theoretical values vary depending on the current-voltage characteristics of the particular diode used. Actual conversion loss values are shown to be higher due to junction capacitance and spreading resistance.

More recently, Saleh [4], extended the foregoing analysis to include what he termed the Z, Y, G and H mixers. In the Y and Z mixers, all the idlers are short circuited and open circuited, respectively. In the G-mixer, the odd-order idlers (including the image) are short circuited and the even-order ones (including the sum product) are open circuited. The reverse is true for the H mixer. It is shown that the optimum conductance waveform for the Y

and Z mixers is a series of pulses, with duty cycle related to the ratio of “on to off” resistances of the diode. The optimum conductance waveform for the G and H mixers is a square wave that is independent of the “on-to-off” resistance ratio. Saleh found the theoretical limit for conversion loss to be 0 dB for all idlers reactively terminated and the image short or open circuited. These four types of mixers are theoretical and are not perfectly realizable in practical circuits.

During the last two decades, computers have increasingly been used to analyze mixers. This approach has obviated the need for many previously required limiting assumptions such as a sinusoidal LO voltage at the diode, constant (linear) diode-junction capacitance, and termination of idlers and LO harmonics in open or short circuits. The general method is to determine the diode conductance waveform resulting from the applied LO, expand this waveform into a Fourier series and relate the resulting harmonics to mixing products through a conversion matrix. The mixer is represented as a linear network with a separate port for each frequency, allowing each

signal to be terminated independently. Maas has given a detailed description of this process [6].

Non-linear microwave CAD programs are available from various companies. Three of these programs were evaluated. One did not successfully converge for a four-diode mixer; however, convergence for a single-MESFET mixer took only one minute, with conversion loss being within 1 dB of measured values. The other two programs were evaluated using the four-diode double-balanced mixer examples supplied with the software. Convergence took about 11 minutes, which resulted in reasonable conversion loss of values.

MIXER PARAMETERS AND OPTIMIZATION

The major goals of mixer design are to minimize conversion loss, noise figure, and intermodulation distortion. Other important parameters to optimize include VSWR and compression.

CONVERSION LOSS

Conversion loss has three major components: RF and IF mismatch loss, loss in the diode spreading resistance, and loss in the diode junction due to junction resistance and generation of IM products. A theoretical example has been given [7] showing that mismatch loss is typically 1 dB or less, but can range from infinite to 0 dB; loss in the spreading resistance is about 1 dB, and loss in the junction is about 4 dB, for a total of 5 to 8 dB in a well-designed mixer.

In double-balanced mixers, the RF input and image signals share the RF port, while the IF and sum products share the IF port. It has been shown that conversion loss can vary up to 2 dB by open or short circuiting the image [8]. This method is used to reduce (enhance) mixer conversion loss. Maas has shown that presenting a short circuit or capacitive termination, to the image provides the best trade-off among conversion loss, noise figure and third-order intermodulation. An open circuit

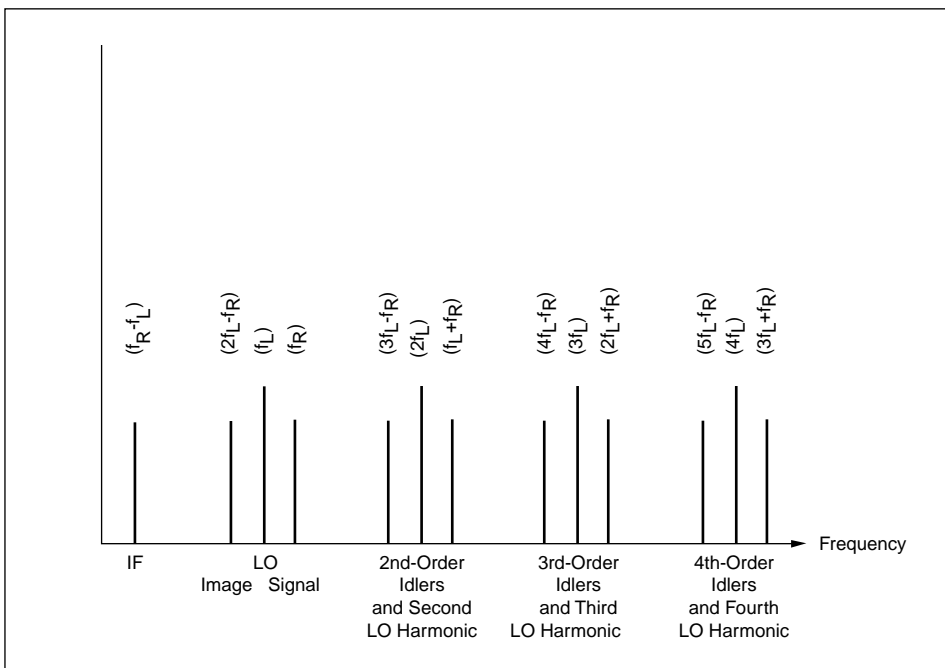


Figure 2. Frequency spectrum of mixing products.

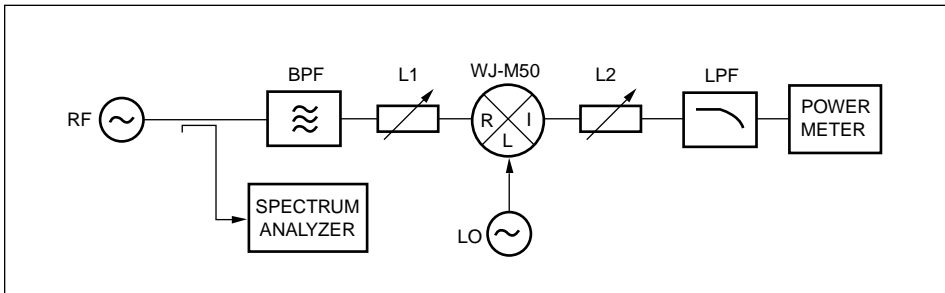


Figure 3. Test setup used to measure conversion loss as a function of Image and sum product terminations.

or inductive image termination can result in significantly degraded noise figure and third-order intermodulation performance [9]. Filtering and phase cancellation [10] have been used to achieve image enhancement, with the filtering method predominant.

Conversion loss can vary by up to 5 dB by simultaneously reactively terminating the $2f_L$, image and sum products [11]. To measure the effect of varying these termination impedances, a broadband mixer which covers 2 to 26 GHz at the RF and LO ports, and 1 to 15 GHz at the IF port, was tested as shown in Figure 3.

Figure 4A shows experimental conversion-loss variation as a function of the line length (L1), which is between the bandpass filter and the RF port of the mixer. The BPF passes the RF but rejects the image and $2f_L$ frequencies. Figure 4B shows conversion-loss variation as a function of the line length (L2), which is between the low-pass filter and the IF-port of the mixer. The LPF passes the IF, but rejects the sum frequency. For this experiment, $f_L = 4.5$ GHz, $f_R = 3.0$ GHz and $f_{IF} = 1.5$ GHz. It was found that for minimum and maximum conversion loss, L1 and L2 are independent of each other. Minimum and maximum conversion loss values for this mixer were found to be about 4.3 dB and 9.5 dB, respectively, excluding filter and variable-line losses.

Results like these show that mixers having conversion loss of 4 to 5 dB or less, must employ enhancement techniques. They also indicate that for swept frequencies, serious conversion-loss ripple can result when filters are placed adjacent to broadband mixer RF or

IF ports. Placing attenuators adjacent to the mixer ports will reduce conversion-loss ripple. Further experimental data shows that ripple can be reduced from 5 dB to approximately 2.5 dB peak-to-peak, at the expense of increasing conversion loss, by placing a 3-dB attenuator at the RF or IF ports of the mixer. Conversion-loss ripple caused by a varying sum-frequency termination, can also be mini-

mized by using a mixer with a low-pass IF port that reflects the sum product energy back into the diodes. Also, filter networks with constant impedance as a function of frequency can be used to control ripple.

The non-cyclical results in Figures 4A and 4B have been reported previously [12] and are attributed to reflections of the second harmonic of the LO, in addition to the image. To test this, the RF and LO frequencies were changed, and the BPF at the RF port was replaced with one that passes the image, but rejects the $2f_L$ product. This resulted in conversion-loss variation as a function of L2 being reduced from 5 dB to 2 dB, and corresponding to variations in the level of the $2f_L$ product exiting the RF port. These results show that the $2f_L$ product termination can be as significant as the image when considering

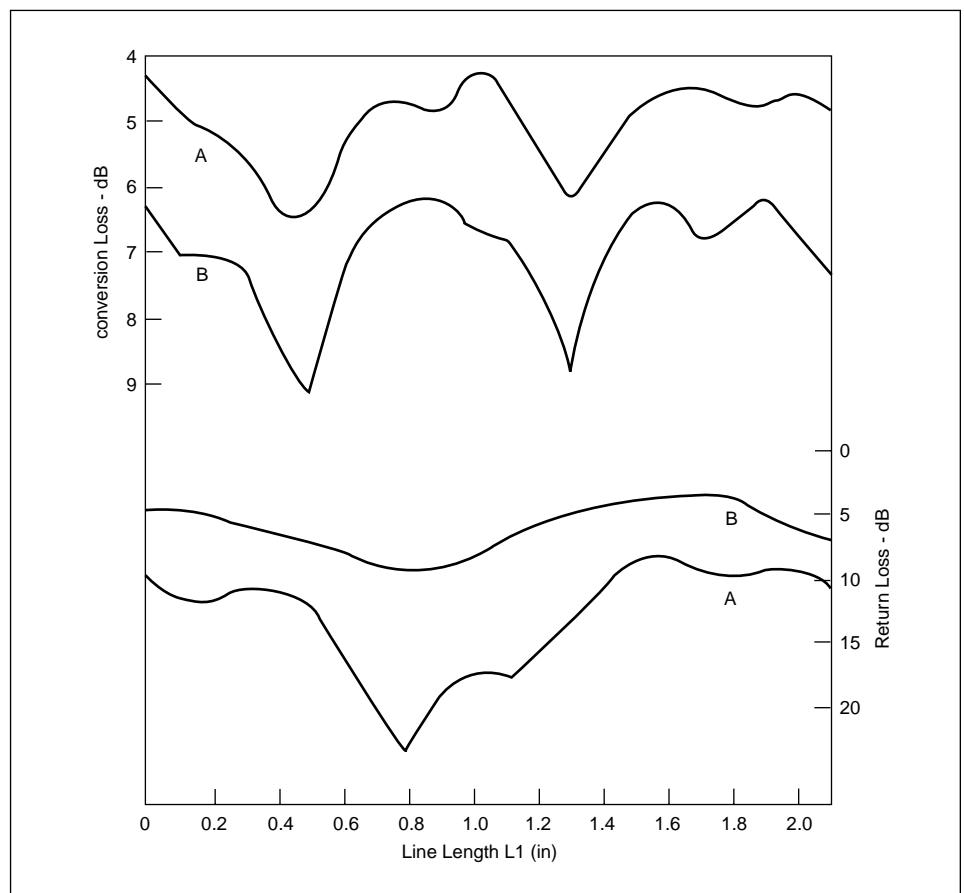


Figure 4A. Conversion loss and R-Port return loss for the test setup shown in Figure 3 as line length, L1, is varied, with L2 set for best (A) and worst-case (B) conversion loss.



conversion-loss enhancement.

NOISE FIGURE

The single sideband (SSB) noise figure is defined as:

$$NF = 10 \log [P_{n \text{ out}} / (P_{n \text{ in}} \times G)] = 10 \log F \quad (4)$$

where,

$P_{n \text{ out}}$ = Available noise output power at IF frequency

$P_{n \text{ in}}$ = Available noise input power at RF frequency

G = Available power gain (algebraic ratio)

F = Noise factor

The SSB noise factor is often described in terms of equivalent input noise temperature, T_{mSSB} [7]:

$$F = 1 + \frac{T_{mSSB}}{T_o} \quad (5)$$

where, $T_o = 290^\circ K$

Noise figure for passive devices is equal to the reciprocal of available power gain, as long as both the noise source and the passive device are at the same temperature. This implies that mixer noise figure equals conversion loss; but, Kerr and others have shown that this is not strictly true: theoretically, mixer noise figure is equivalent to that of an attenuator having effective noise temperature T_M equal to $nT/2$, where n is the diode ideality factor and T is the diode physical temperature. This results in noise factor for a SSB mixer, one having infinite image conversion-loss, being given as [6]:

$$T_{mSSB} = (nT/2) (L-1) \quad (6)$$

where L is algebraic RF-to-IF conversion-loss. This is true for an ideal mixer in which all idler frequencies are reactively terminated. However, actual mixer noise factor values tend to be higher, in part due to partial correlation of down-converted shot-noise power, which is generated by the time varying diode series resistance.

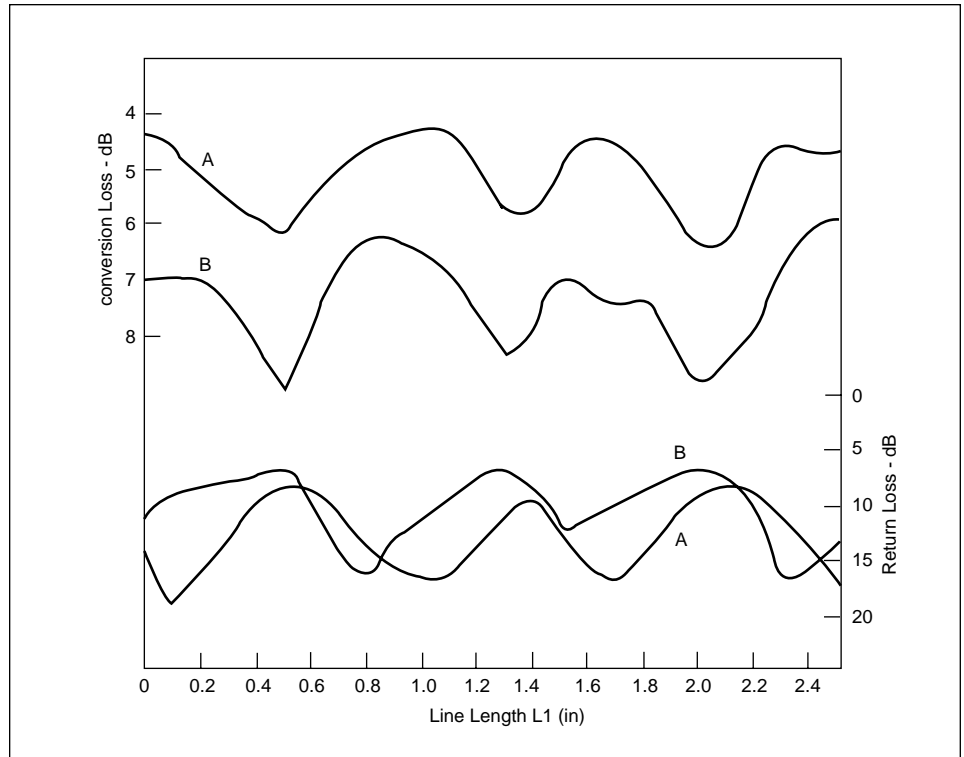


Figure 4B. Conversion loss and R-Port return loss for the test setup shown in Figure 3 as line length, L2, is varied, with L1 set for best (A) and worst-case (B) conversion loss.

The predominant sources of noise in Schottky diodes are thermal (Johnson) noise in the series resistance, shot noise generated by current flow across the barrier [7] and flicker (1/f) noise. Thermal noise is generated by random current fluctuations in any resistor with no external voltage present. Shot noise results from a stream of electrons moving through the diode barrier at random velocities, while producing an average dc current. Thermal noise is a limiting form of shot noise with zero bias applied.

Flicker noise is present in many devices, including carbon resistors and silicon diodes when current is flowing in them. For low frequencies (below approximately 1 MHz), flicker-noise power is approximately proportional to $1/f$, where f is the operating frequency [13]. Flicker noise in a Schottky diode is related to surface-state density [14].

In addition to the above mechanisms of noise generation, noise may become present at the mixer output due to reciprocal mixing, cross

modulation and imperfect LO-AM rejection. Reciprocal mixing causes noise present on the LO signal to be transferred to the IF output when a second RF input at a high level becomes present at the mixer RF input [15]. Rejection of AM noise on the LO is achieved in balanced mixers in the same manner as L-to-I isolation. Phase noise on the LO, however, is directly transferred to the IF signal. The magnitude of the peak phase deviation is multiplied

in harmonic mixers by the LO harmonic number.

INTERMODULATION

Intermodulation (IM) distortion causes output products to be generated at frequencies of:

$$f = \pm nf_L \pm m_1 f_{R1} \pm m_2 f_{R2} \pm \dots \quad (7)$$

where n, m_1, m_2, \dots are integers. The value, n , is called the order of modulation, while the sum ($|m_1| + |m_2| + \dots$) is referred to as the order of intermodulation. As shown by equa-

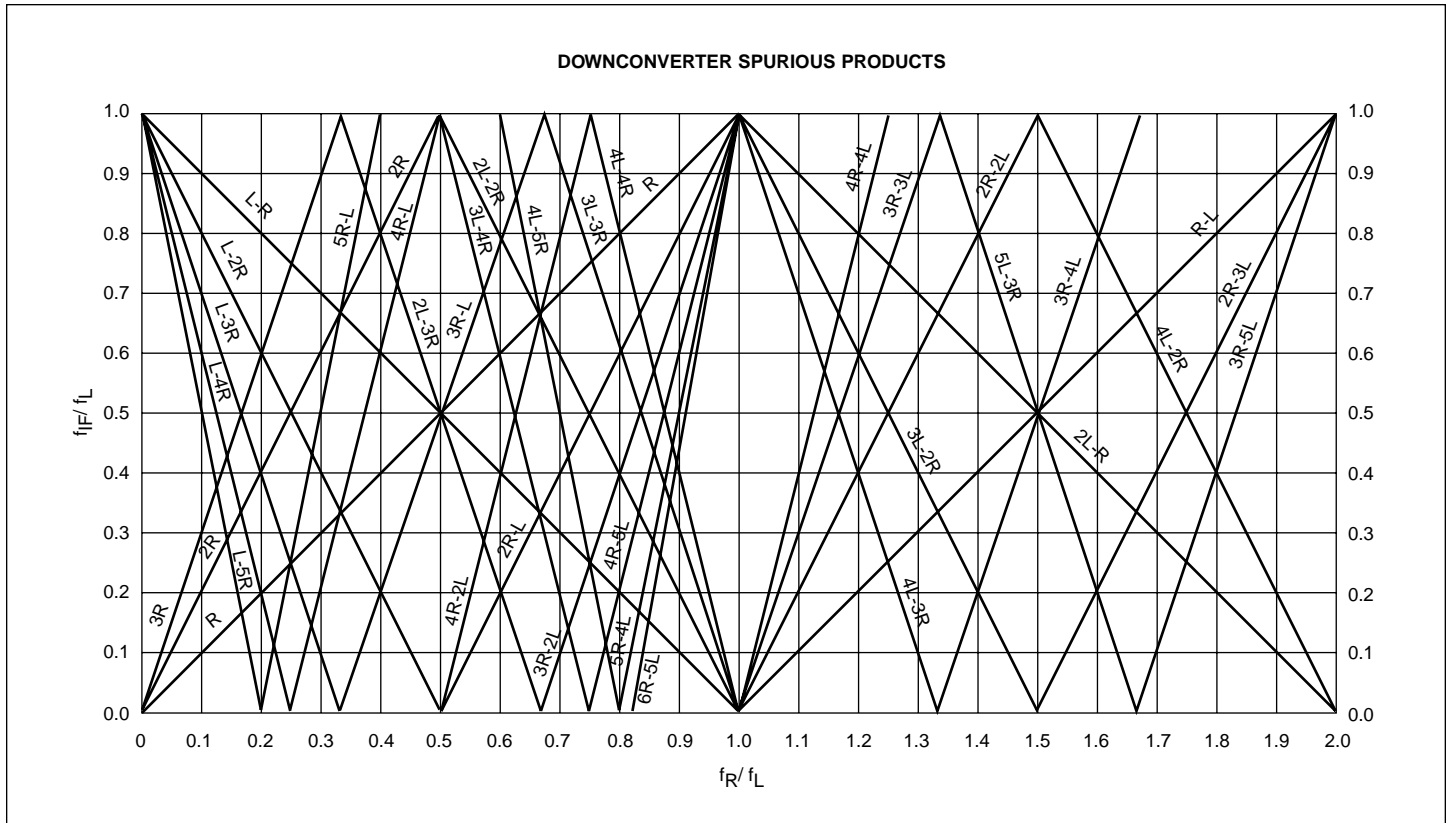


Figure 5A. Downconverter spurious products chart.

tion 1, the linear square-wave phase-reversal mixer generates IM products with frequencies of $f = nf_L \pm f_R$. IM products with intermodulation orders greater than one are generated by incremental diode nonlinearity and overloading, and can be considered nonlinear IM products [16]. Overloading in diode mixers occurs as the RF signal level approaches the LO level, causing switching time to become a function of RF as well as LO voltage.

It is important to identify the IM products present in the IF output passband. This is easily done in a graphical manner for single-tone products using charts such as those shown in Figures 5A and 5B, which are for down- and up-conversion, respectively. An example of their usage is given in Appendix A. Computer-generated IM search programs are also very helpful in identifying the frequencies of IM products [6,17].

IM suppression for single and two-tone prod-

ucts are generally of most interest. The order of intermodulation is important because it describes the behavior of the relative suppression between the IM and IF products as the RF input power is varied. For example, the two-tone, third-order IM product at $f = f_L + 2f_{R1} - f_{R2}$, for $P_{RF1} = P_{RF2} \ll P_{LO}$, varies 3 dB for every 1 dB of variation in the IF product as P_{RF1} and P_{RF2} are varied. This behavior generally applies to all orders of intermodulation for any number of input tones. It gives rise to the concept of input intercept point, which equals the extrapolated input power to the mixer (at each tone) that would cause the output power levels of the IM and IF products to become equal. The benefit of using the intercept method is that instead of having to state both the input power level and relative level of suppression, only the intercept point needs to be stated because suppression is assumed to be 0 dB. Input intercept is given by:

$$3IIP \text{ (dBm)} = \frac{\text{Suppression}}{(\text{IM order}-1)} + P_{RF \text{ in}}$$

where:

$$P_{RF \text{ in}} = \text{Input RF Power for each tone; in dBm.} \tag{8}$$

For example, the two-tone, third-order input intercept point for a mixer with $P_{RF1} = P_{RF2} = -10$ dBm, and relative suppression of 60 dBc, is:

$$3IIP = [60/(3-1)] - 10 = + 20 \text{ dBm} \tag{9}$$

Output intercept point equals input intercept point plus device available power gain. It can be shown that the theoretical third-order input intercept point caused by overloading in the linear phase-reversal mixer is equal to P_{LO} (dBm) + 9.0 dB [2]. In practice, the third-order input intercept point for diode mixers ranges from about 0 to 5 dB above the LO power. It is higher for passive MESFET mixers because the FET conductance waveform is more linear, and overloading is mini-

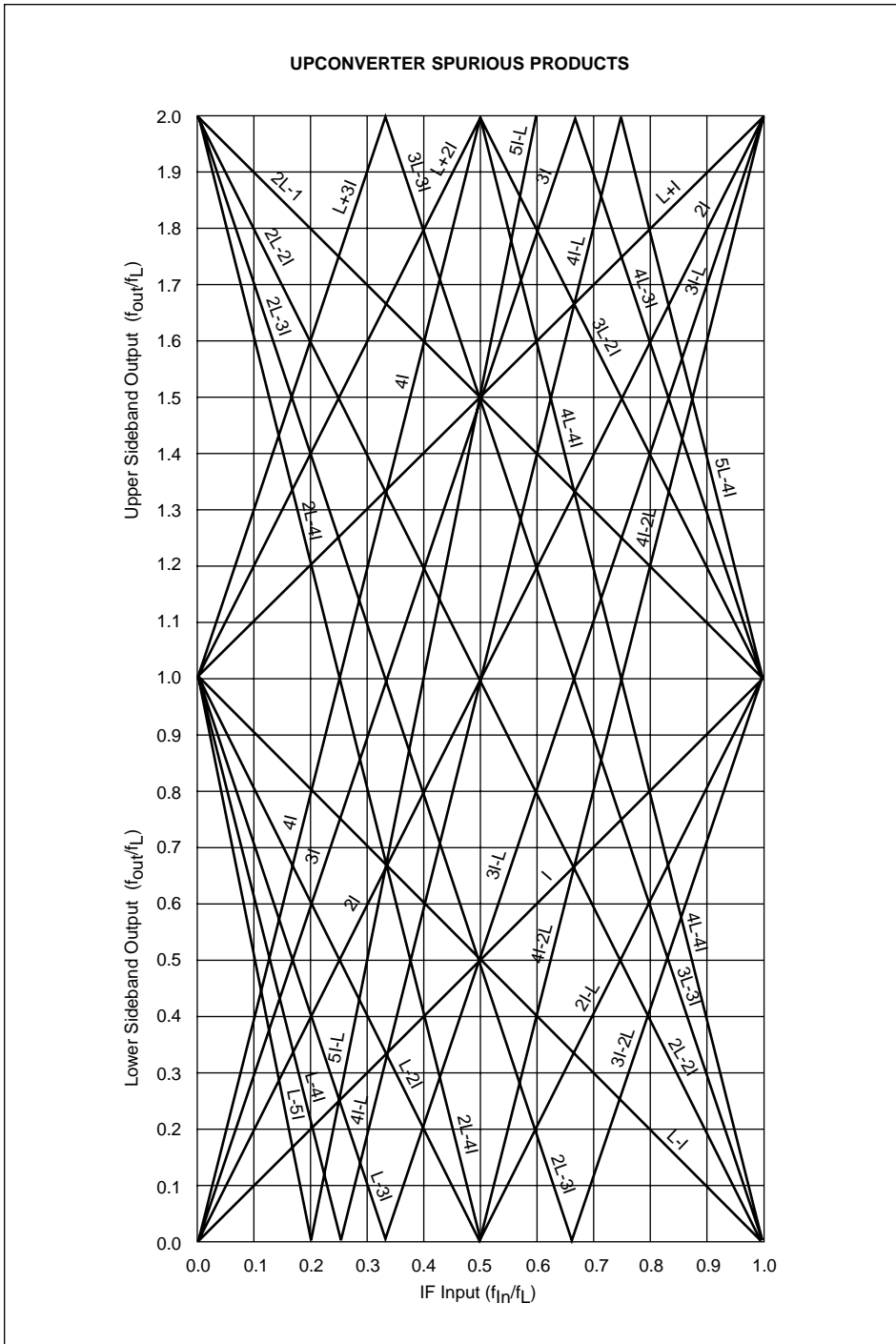


Figure 5B. Upconverter spurious products chart.

mized by separating the RF and LO voltages so that high RF levels are less able to phase modulate the conductance waveform [18,19,20]. Since overloading is caused by the interference of the RF signal with the LO, its

effects can be reduced by using a square-wave LO, assuming the RF voltage level remains below that of the LO. IM suppression caused by overloading in a double-balanced mixer has been given for various products as a func-

tion of diode and circuit imbalance [21].

Non-linear intermodulation can be reduced by placing a resistor in series with each mixer diode, thus, reducing its overall non-linearity [22]. Also, placing two diodes in series or in parallel reduces intermodulation. Various classes of mixers with these configurations have been described by Cheadle, and are given in Figure 6.

CROSS MODULATION

Cross modulation is the process whereby modulation or noise that is present on an adjacent strong RF input signal is made to appear on the IF output signal. This is similar to reciprocal mixing, in which the noise originates from the LO signal. A method of computing cross modulation levels has been given by Gretsch [23].

Part 2 of Mixers in Microwave Systems will discuss such topics as impedance matching, diode-mixer design, mixer realization, and use of mixers.

APPENDIX A: IM CHART EXAMPLES

Use of Figures 5A and 5B is straightforward. These charts comprise the family of lines:

$$f'_{OUT} = n + m f'_{IN}$$

Where f'_{OUT} and f'_{IN} are the output and input frequencies, respectively, normalized by the LO frequency. In Figure 5A the L-R and R-L lines represent the transfer functions for input-to-output frequency for the IF product when $f_R < f_L$ and $f_L < f_R$, respectively. The goal is to determine which IM products will appear within the IF passband for given values of f_{IF} , f_R and f_L . For example, when $f_R = 6$ to 8 GHz, $f_L = 10$ GHz and $f_{IF} = 2$ to 4 GHz, a square is drawn on the L-R line with corners corresponding to the points $f'_{IN} = 0.6$ and 0.8. The 2R-L and 3R-2L lines cut through this box, so that when $f'_{IN} = 0.6$, we see that $f'_{2R-L, OUT} = 0.2$, and when $f'_{IN} = 0.8$, $f'_{3R-2L} = 0.4$, corresponding to output frequencies of 2 and 4 GHz, respectively.



MIXER CLASS	CIRCUIT	LO POWER FOR DB MIXERS (dBm)
Class 1		+7 to +13
Class 2, type 1		+13 to +24
Class 2, Type 2		+13 to -24
Class 3, Type 1		-20 to +30
Class 3, Type 2		+20 to +30
Class 3, Type 3		+20 to +30

Figure 6. The various classes of mixer-diode configurations.

As f_R increases to 8 GHz, the L-R IF product decreases in frequency while the 2R-L and 3R-2L products increase in frequency, traversing the 2 to 4 GHz IF passband at two and three times, respectively, the rate of the IF frequency shift. The up-conversion chart in Figure 5B is used in the same manner.

ACKNOWLEDGEMENT

The author wishes to thank S.E. Avery, Dr. R.K. Froehlich, and Dr. R.G. Ranson for their thoughtful review of this paper, M.A. O'Mahoney, and T.G. Skala for their non-linear CAD evaluations, R.W. Bruce for the usage of his extensive bibliography, and R.Y.S. Parsons for preparing the draft.

REFERENCES

1. Tucker, D.G. "The Input Impedance of Rectifier Modulators," IEE Proc., Vol. 107B, No. 1, pp. 273-284, January 1960.
2. Gardiner, J.G., et al. "Distortion Performance of Single-Balanced Diode Modulators," IEE Proc., Vol. 117, No. 8, August 1970.
3. Kelly, A.J. "Fundamental Limits on Conversion Loss of Double Sideband

- Resistive Mixers," IEEE Trans. Microwave Theory Tech., Vol. MTT-25, No. 11, November 1977, pp. 867-869.
4. Saleh, A.A.M. Theory of Resistive Mixers, Cambridge, Massachusetts: MIT Press, 1971.
5. Torrey, H.C. and CA. Whitmer. Crystal Rectifiers, New York: McGraw-Hill, 1948
6. Maas, S.A. Microwave Mixers, Artech House, Dedham MA, 1986.
7. Held, D.N. and AR. Kerr. "Conversion Loss and Noise of Microwave and Millimeter-Wave Mixers: Part 1-Theory and Part 2-Experiment," IEEE Trans. Microwave Theory Tech., Vol. MTT-26, No.2, February 1978.
8. Burkley, C.J. and R.S. O'Brien. "Optimization of an 11 GHz Mixer Circuit Using Image Recovery," Int. J. Electron, Vol. 38, pp. 777-787, June 1975.
9. Mass, S. "Two-Tone Intermodulation in Diode Mixers," IEEE Trans. Microwave Theory and Tech., Vol. MTT-35, No. 3, March 1987, pp. 307-314.

10. Oxley, T.H. "Phasing Type Image Recovery Mixers," IEEE MTT-S mt. Microwave Symposium Digest, pp. 270-273, 1980.
11. Dickens, L.E. and D.W. Main. "An Integrated-Circuit Balanced Mixer, Image and Sum Enhanced," IEEE Trans. Microwave Theory Tech., Vol. MTT-23, No. 3, March 1975.
12. Pound, R.V. Microwave Mixers. Usington, Massachusetts: Boston Technical Publishers, Inc., pp. 81-87, 1964.
13. Shurmer, H.V. Microwave Semiconductor Devices. New York: Wiley Interscience, 1971.
14. Sze, SM. Physics of Semiconductor Devices. New York: Wiley Inter-science, 1969, p. 459.
15. Sabin, WE. and E.O. Schoenike. Single-Sideband Systems and Circuits, New York: McGraw-Hill, 1987.
16. Steinbrecher, D.H. "Mixer Fundamentals," Notes presented at 1989 RF Technology Expo, Santa Clara, CA.
17. Barn, R. "A Mixer Spurious Plotting Program," RF Design, May 1989, pp. 32-43.
18. Weiner, S., D. Neuf and S. Spohrer. "2 to 8 GHz Double Balanced MESFET Mixer with +30 dBm Input 3rd Order Intercept," IEEE MTT-S mt. Microwave Symposium Digest, pp. 1097-1100, 1988.
19. Maas, SA. "A GaAs MESFET Mixer With Very Low Intermodulation," IEEE Trans. Microwave Theory Tech., Vol. MTT-35, No. 4, April 1987.
20. Oxner, E. "A Commutation Double-Balanced MOSFET Mixer of High Dynamic Range," Proceedings 1986 RF Expo East, pp. 73-87.
21. Henderson, B.C. "Reliably Predict Mixer IM Suppression," Microwaves and RF, Vol. 22, No. 12, Nov. 1983.



22. Cheadle, DL. "Consider a Single Diode to Study Mixer Intermod," *Microwaves*, Dec. 1977.
23. Grets, W.R. "The Spectrum of Intermodulation Generated in a Semiconductor Diode Junction," *Proc. IEEE*, Vol. 54, No. 11, November 1966.
24. Faber, MT. and W.K. Gwarek. "Nonlinear-Linear Analysis of Microwave Mixer With Any Number of Diodes," *IEEE Trans. Microwave Theory Tech.*, Vol. MTT-28, No. 11, Nov. 1980.
25. Mouw, RB. "A Broad-Band Hybrid Junction and Application to the Star Modulator," *IEEE Trans. Microwave Theory Tech.*, Vol. MTT-16, pp. 911-918, Nov. 1968.
26. Henderson, B. "Orthogonal Mixers: Punching Up Earth/Space Payload Performance," *MSN- January 1982*, Vol. 12, No. 1.
27. Will, P. "Termination Insensitive Mixers," *Professional Program Session Record 24, WESCON, San Francisco, 1981*.
28. Norton, D. "Three Decade Bandwidth Hybrid Circuits," *Microwave Journal*, Vol. 31, No. 11, Nov. 1988, pp. 117-126.
29. Henderson, B. and J. Cook. "Image Reject and Single Sideband Mixers," *MSN*, Vol. 17, No. 9, August 1987.
30. Aikawa, M. and H. Ogawa. "Double Sided MIC's and Their Applications," *IEEE Trans. Microwave Theory Tech.*, Vol. 37, No. 2, February 1989.
31. Hirota, T., Y. Tarusawa and H. Ogawa. "Uniplanar MMIC Hybrids A Proposed New MMIC Structure," *IEEE Trans. Microwave Theory Tech.*, Vol. 37, No. 2, February 1989.
32. Izaclian, J., et al. "A Uni-Planar Double-Balanced Mixer Using A New Miniature Beam Lead Crossover Quad," *IEEE mt. Microwave Symposium Digest*, pp. 691-694, 1988.
33. Pavio, AM., et al. "Double Balanced Mixers Using Active and Passive Techniques," *IEEE Trans. Microwave Theory Tech.*, Vol. 36, No. 12, December 1988.
34. Titus, W., et al. "Distributed Monolithic Image Rejection Mixer," *IEEE Int. GaAs IC Symposium*, pp. 191-194, 1986.
35. Ali, F, S. Moghe and R. Ramachandran. "A Highly Integrated X-Ku Band Upconverter," *IEEE GaAs IC Symposium Digest*, pp. 157-160, 1988.
36. Private communication with AF. Podell.
37. Fotowat, A. and E. Murthi. "Gilbert-Type Mixers vs. Diode Mixers," *Proceedings RF Technology Expo 1989*, pp. 409-413.
38. Wilson, SE. "Evaluate The Distortion of Modular Cascades," *Microwaves*, Vol. 20, March 1981.
39. Sorger, G.U. "The 1 dB Gain Compression Point for Cascaded Two-Port Networks," *Microwave Journal*, July 1988.
40. Avery, SE. "Dual Mixers," *Watkins-Johnson Company Tech-notes*, Vol. 13, No. 4, July/August 1986.
41. Schindler, SA. "MIL-Specification Mixers," *Watkins Johnson Company Tech-notes*, Vol. 15, No. 2, March/April 1988.

Note: Many of the referenced articles appear in the following volume of IEEE Press Selected Reprint Series: EL. Kollberg, "Microwave and Millimeter-Wave Mixers," IEEE Press, New York, N.Y., 1984.